EFFECT OF THE FLOW RATE ON AN IMBIBITION CAPILLARY PRESSURE CURVE: THEORY VERSUS EXPERIMENT

François Kalaydjian
Institut Français du Pétrole, Rueil-Malmaison, France

Abstract Dynamic capillary pressure measurements have been performed during waterfloods, at various flow rates. The capillary pressure is shown to be flow rate dependent: it increases with the flow rate and its derivative with respect to saturation mostly decreases when the flow rate is increased. These dynamic capillary pressure measurements have been used to interpret the flow experiments and calculate the relative permeabilities. Relative permeabilites were found to increase with the flow rate. These results cannot be interpreted in the standard framework of modelling two-phase flow in porous media. A new model, based on an averaging technique is presented.

INTRODUCTION

In the standard approach to two-phase flow in porous media, it is assumed that the flow parameters depend only on the saturation. This approach is based on two main features: the notion of capillary pressure and the notion of relative permeabilities. The notion of capillary pressure is a generalization of the Laplace law, which is only valid under static conditions. The generalized Darcy equations relate the flow velocity of each phase to the pressure gradient in this phase and involve the notion of relative permeabilities. The relative permeabilities express the reduction of flow paths offered to a phase due to the presence of the other phase.

Therefore, in the standard approach, these flow parameters are assumed to be functions only of saturation.

In the standard framework, viscous effects are taken into account in the definition of the relative permeabilities and the capillary pressure reflects all the capillary effects in the displacement of the two phases. Many attempts to verify whether this standard framework was valid or not, have been carried out in the literature. For instance, relative permeabilities have been found to depend on wettability (Dullien *et al.*, 1990), and viscosity ratio (Danis and Jacquin, 1983). As well, relative permeabilities have been shown to depend on the flow rate, in fact on the ratio of the capillary forces to the viscous forces (Kalaydjian and Bourbiaux, 1989; Kalaydjian, 1990). Finally, dynamic effects have been claimed to modify capillary parameters, such as the contact angle (Ngan and Dussan, 1982; Calvo *et al.*, 1991).

In this paper, the effect of the competition between the viscous and the capillary forces on capillary pressure is studied to establish whether or not capillary pressures measured during displacement are modified by the flow conditions.

This paper is organized as follows. In the first part, the experimental device and the experimental results concerning the capillary pressure measurements and relative permeabilities measured during a series of waterfloods performed in two outcrop rock samples, a limestone and a sandstone, are presented. In the second part, the method used to derive a new expression for the capillary pressure is presented briefly. The new model is verified by comparison with the experimental data.

EXPERIMENTS

Experimental Device

Two series of waterflood tests have been performed in two different kinds of water wet rock: a limestone (sample L13) and a sandstone (sample M5500). The petrophysical characteristics of each sample are given in Table 1. The characteristics of the fluids which have been used are presented in Table 2.

TABLE 1 Petrophysical parameters

Property*	L13	M5500
ϕ (%)	26.7	22.91
k (m^2)	$163\ 10^{-15}$	$174\ 10^{-15}$
L(m)	0.222	0.242
A (m2)	$10.15\ 10^{-4}$	$11.16\ 10^{-4}$

TABLE 2 Characteristics of the fluid phases

Property*	Aqueous phase	Oil phase
μ (Pa.s)	$1.0437\ 10^{-3}$	$1.49\ 10^{-3}$
d ($g.cm^{-3}$)	0.758	1.032

Porosity profiles for each sample have been determined by use of a gammametry technique with the same device described in (Kalaydjian and Bourbiaux, 1990). These measurements show a relatively homogeneneous porosity of the two porous media, especially for the sandstone sample (the porosity of sample L13 is shown in Figure 1)

The two samples were positioned vertically, their sides coated with epoxy resin and were equipped with four pairs of pressure transducers positioned on opposite sides of the sample and fitted with semi-permeable membranes made of water wet or oil wet filter paper (0.22 μm in pore radius and 125 μm in thickness). At the beginning of the experimental procedure, the porous media were fully saturated with water. Use of pressure taps enabled the determination of absolute permeabilities in portions of the medium contained between two pressure taps. This allowed verification that the media were relatively homogeneous with respect to the absolute permeability.

* Nomenclature: at end of paper

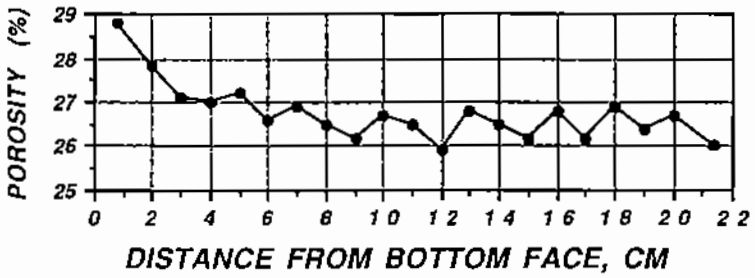

FIGURE 1 Porosity profile, sample L13

Then, in a plane perpendicular to the one containing the pressure taps, fifteen pairs of ultrasonic transducers were positioned along two opposite sides of the core. In particular, four of them were placed at the same levels as the pressure transducers. This device, represented in Figure 2, allowed simultaneous in-situ measurement of the saturation profiles, the pressure drops in both phases, the recovery and the total pressure drop during a flow test.

Since at several locations along the core the water and oil pressures were measured together with the saturations (time constant of pressure measurements being instantaneous, membranes having 125 μm in thickness), it was possible to determine under dynamic conditions, the capillary pressure curve by taking the difference between the two pressures and relate it to the saturation measurement.

Typically a waterflood test consisted of the following steps: (1) fully saturating the core with water, (2) performing an oil drainage from the top down in order to establish the initial oil saturation and finally (3) performing a waterflood from the bottom up. All the operations were fully automatic.

In order to measure the saturations, an ultrasonic method (Bacri and Salin, 1989, Hoyos *et al.*, 1990) consisting in measuring the flight time of an ultrasonic wave between two transducers across the porous medium was used. In order to come up with a saturation measurement, it was necessary to calibrate the method. This has been done by comparison with saturation measurements performed with an X-ray CT-

scanner. The accuracy expected of this method is about 2% saturation, according to Deflandre *et al.*, 1992.

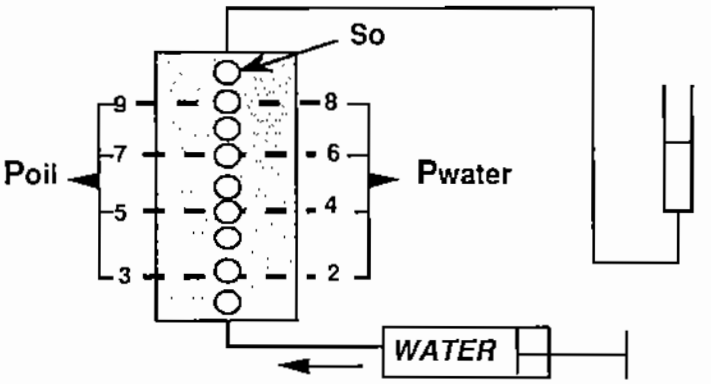

FIGURE 2 Scheme of the experimental device

Experimental results

On sample L13 as well as on the sandstone sample M5500, a series of three waterflood tests were performed at various flow rates: 1, 5 cc/hr and 15 cc/hr. Water was injected from the bottom end in order to avoid any flow instabilities. For each of these tests, end points of water relative permeabilities (cf Table 3), saturation profiles, recovery, total pressure drop and the pressures in both phases have been recorded.

TABLE 3 End points of water relative permeabilities

k_{rw} @ S_{or}	1 cc/hr	5 cc/hr	15 cc/hr
L13	0.074	0.091	0.095
M5500	0.045	0.040	0.029

The three series of measured saturation profiles for sample L13 are presented in Figure 3 (a,b,c).

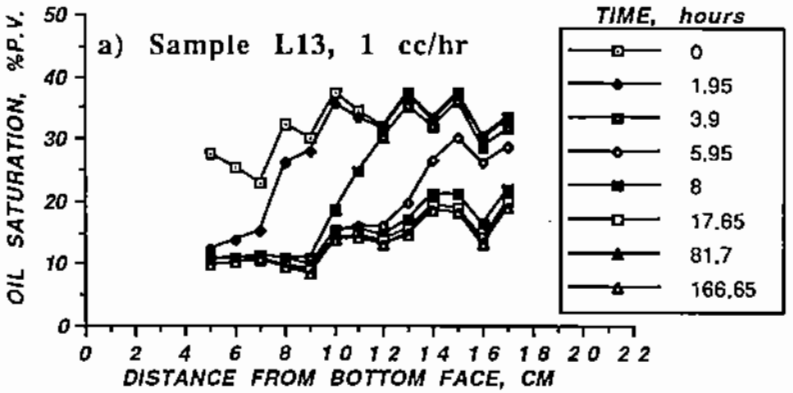

FIGURE 3A Measured saturation profiles (1 cc/hr)

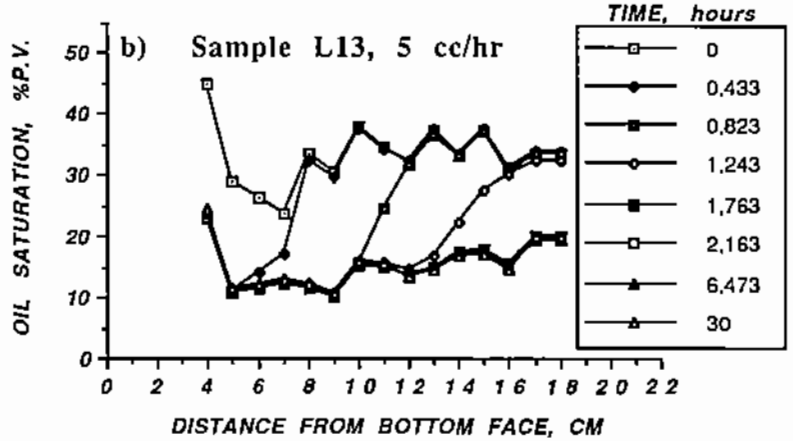

FIGURE 3B Measured saturation profiles (5 cc/hr)

Average initial and final oil saturations were similar in the

three tests (Table 3) within the accuracy of the method. They were taken as identical for the three waterflood tests.

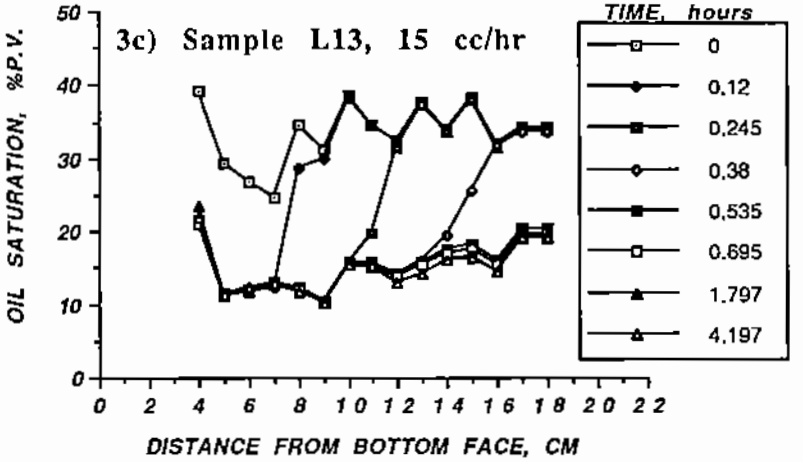

FIGURE 3C Measured saturation profiles (15 cc/hr)

For the limestone sample L13, the initial oil saturation S_{oi} was obtained by oil/water drainage and was equal to 38%, while the residual oil saturation S_{or} was 18%. This narrow variation of mobile saturation was due to the limitation in the pressures (maximum 1,000 hPa) that could be imposed in the experiment.

Pressures in both fluid phases were measured during the experiments. As these experiments were globally unidirectional - the saturation is supposed to be uniform in a normal section -, the difference between the pressures measured at the same level, in the oil and the water phase respectively, was defined as the capillary pressure. The variations of saturation at the same level were recorded as well. It was then possible to relate capillary pressure and saturation measurements performed at the same time and at the same location along the axis of the porous medium. This procedure led to the determination of capillary pressure

curves, locally and under dynamic conditions. In Figure 4(a) the capillary pressure curves measured at the level where the value of the permeability was closest to the average value, are presented for the different waterflood tests in both samples.

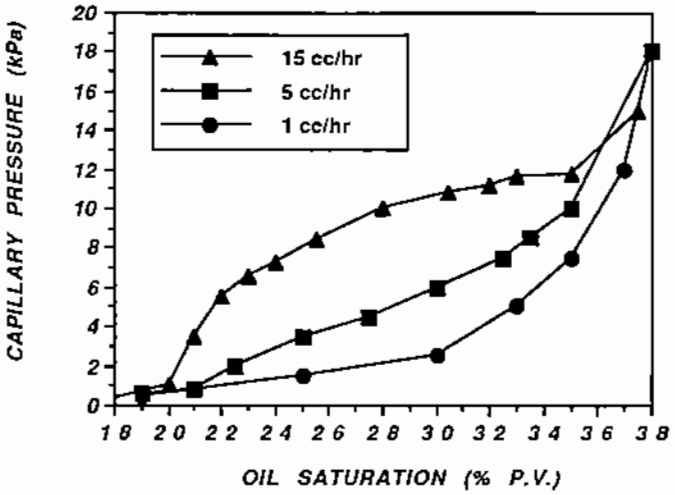

FIGURE 4A Dynamic capillary pressure curves (L13)

The same procedure was used to study waterfloods performed in the sandstone sample M5500. The same trend has been observed for the capillary pressure measured under dynamic conditions (Figure 4b): the higher the flow rate, the higher the capillary pressure and the lower the capillary pressure derivative with respect to saturation.

The evolution of the saturation during a two-phase flow test involves the derivative of the capillary pressure with respect to saturation. The capillary effects are thus taken into account through the capillary pressure gradient $\partial P_c/\partial x$.

To find by experiment that when the flow rate is increased this tends to decrease the capillary pressure gradient would be consistent with a decreasing impact of capillary effects on the flow processes.

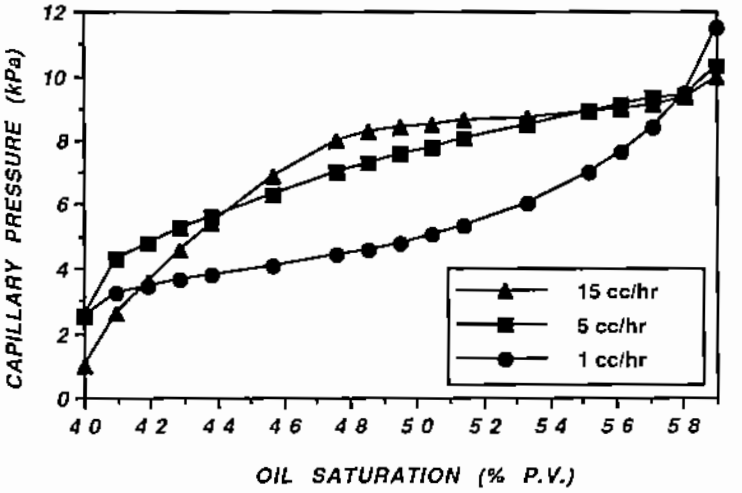

FIGURE 4B Dynamic capillary pressure curves (M5500)

Moreover, the increase in capillary pressure can be explained by evoking purely dynamic effects. It has been shown (Legait *et al.*, 1983) that due to viscous effects, a water/oil meniscus could jump a series a throat sizes otherwise inaccessible under quasi-static conditions.

This constitutes the so-called Haines jumps. Now, due to this effect, we must expect, for a given capillary pressure, under dynamic conditions a greater wetting phase saturation than under quasi-static conditions as shown in Figure 5.

If this interpretation holds, the alteration of the capillary pressure will depend on the structure of the porous medium because the increase of saturation in pores that are accessible to the meniscii is closely related to the coordination number and the pore-to-pore and pore-to-throat correlations as it appears in the modelling of capillary pressure experiments (Tsakiroglou and Payatakes, 1991).

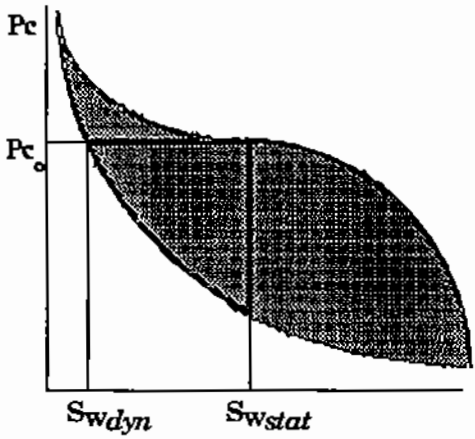

FIGURE 5 Interpretation of changes of the capillary pressure curve due to local dynamic effects

Calculation of the relative permeabilities

In order to complete the interpretation of these experiments, the relative permeabilities have been calculated for each flow rate. The experimental capillary pressures have been used. The relative permeabilities have been found using a programmed fitting procedure, by the best fit to the saturation profiles, the recovery curve and the total pressure drop, and the experimental capillary pressure curves. The software FISOLE developed jointly at IFP and at INRIA (Chardaire *et al.*, 1989) was used. A comparison between experimental and calculated recovery curves is shown in Figure 6(a,b,c) hereunder.

In Figure 7, similar comparison is shown at the two high flow rates (5 and 15 cc/hr) for the total pressure drop. A good agreement has been obtained, too. Finally, for the low flow rate test, the good agreement between experimental and calculated saturation profiles can be observed by comparing Figure 8 to Figure 3a.

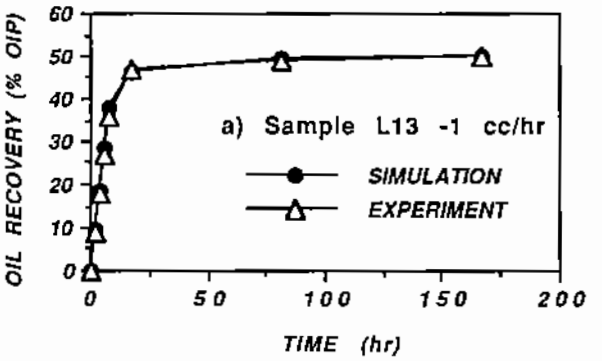

FIGURE 6A Comparison between experimental and calculated recovery curves (1 cc/hr)

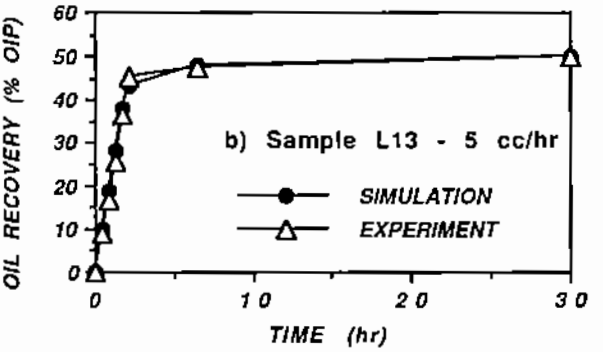

FIGURE 6B Comparison between experimental and calculated recovery curves (5 cc/hr)

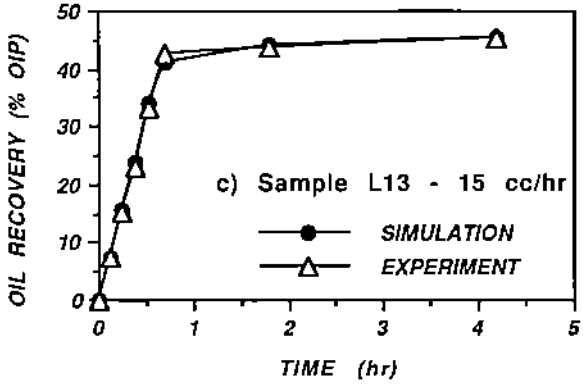

FIGURE 6C Comparison between experimental and calculated recovery curves (15 cc/hr)

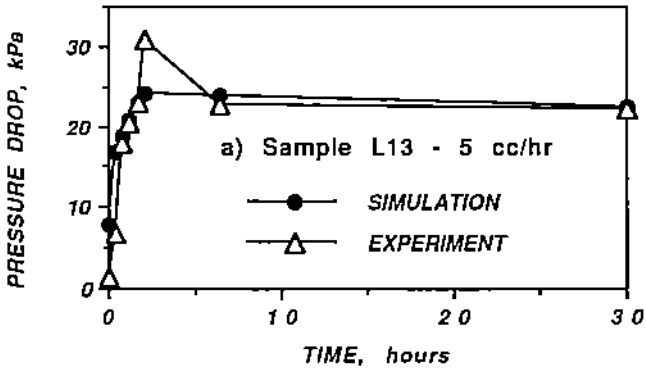

FIGURE 7A Comparison between experimental & calculated pressure drops (5 cc/hr)

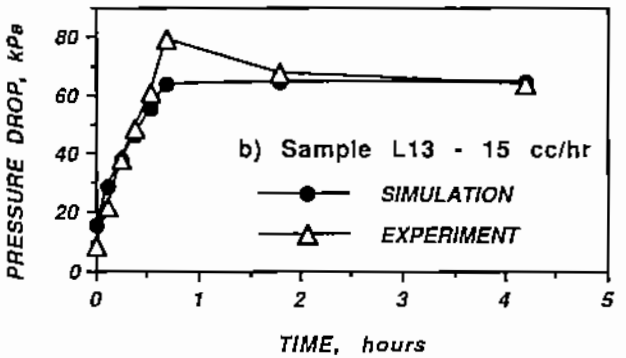

FIGURE 7B Comparison between experimental and calculated pressure drops (15 cc/hr)

These comparisons confirm the consistency of the experimental data and the calculated relative permeabilities (see Figure 9).

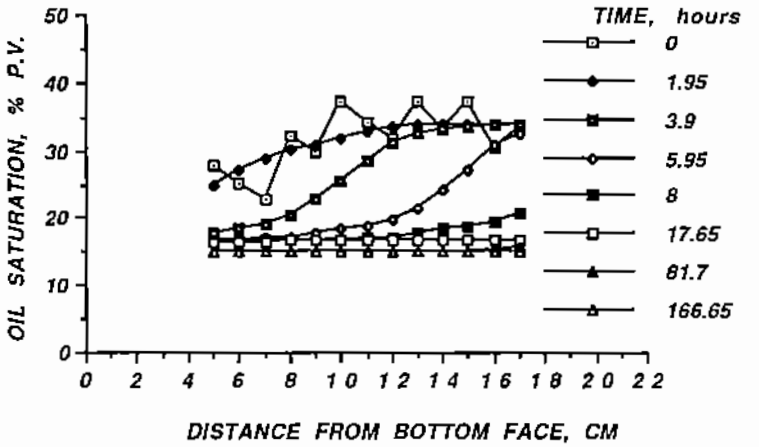

FIGURE 8 Calculated saturation profiles (1 cc/hr)

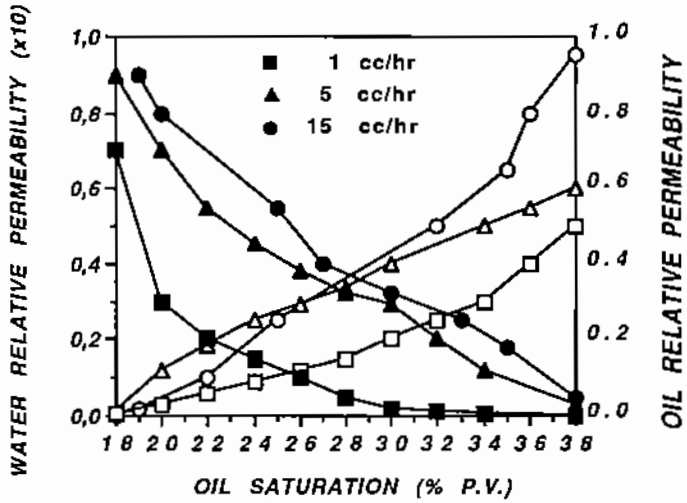

FIGURE 9 Relative permeabilities vs flow rate

In addition, very good agreement between the experimental and calculated end points of relative permeabilities has been found.

According to these curves, it is clear that relative permeabilities depend on the flow rate, in fact on the capillary number defined as the ratio of the viscous forces to the capillary forces: the higher the capillary number, the higher are the relative permeabilities. More precisely, by increasing the flow rate from 1 cc/hr to 15 cc/hr, the end-point of water relative permeability has been increased by 30% and the end-point of oil relative permeability by 40%. Another observation can be made: by increasing the flow rate, and thus the capillary number, the curvature of the relative permeabilities is vanishing: relative permeabilities are straight lines. The changes in the relative permeabilities due to increasing flow rates are even more dramatic at intermediate saturation values. For instance, at S_0=26%, the water relative permeability has increased from 0.01 (1cc/hr) to 0.045 (15 cc/hr), which corresponds to increase of 400%. At So=30%, the oil relative permeability has increased from 0.20 (1cc/hr) to 0.42 (15 cc/hr) that is an increase of more than 100%.

The effect of dynamic capillary pressure curves on relative permeabilities has been investigated by comparing the results of calculations performed using quasi-static capillary pressure curves and dynamic capillary pressure curves. The relative permeabilities were found by fitting to the recovery curve and the total pressure drop. These calculations have been carried out for the flow test performed at 5 cc/hr (Figure 10). It is noticed that for the curves determined with the quasi static capillary pressure, the end-point of water relative permeability exceeds the experimental value: the calculated value was 0.12 while the experimental value was 0.09. The oil relative permeability end-point changes from 0.6 to 0.8.

In addition, the curves are displaced and their curvatures are different. The curvatures of the curves calculated with the quasi-static capillary pressure are less than those of the the curves calculated with the dynamic capillary pressure. This is as if there was a transfer of capillarity effects between the capillary pressure curve and the relative permeability curves.

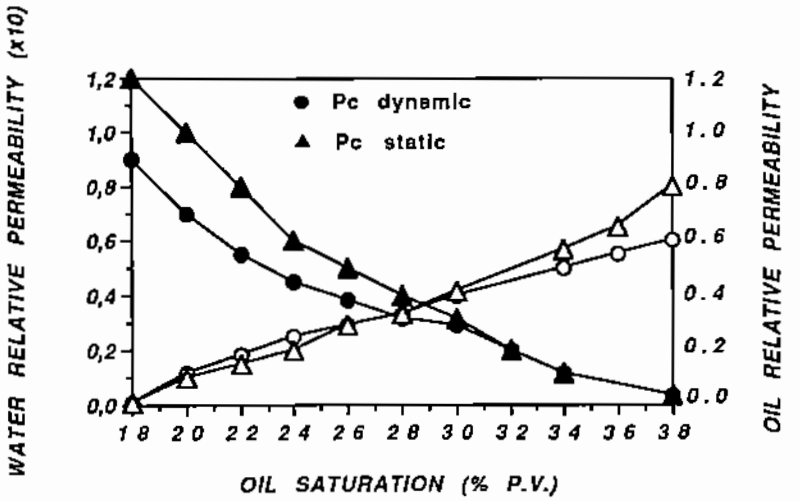

FIGURE 10 Effect of the choice of the capillary pressure (dynamic/static) on the relative permeabilities (5 cc/hr, L13)

Capillary effects are overestimated by the quasi-static capillary pressure curve and as a result, the relative permeabilities show smaller capillary effects which is reflected by lower curvatures of the relative permeabilities.

These results show the importance of measuring dynamic capillary pressures in order to obtain correct relative permeabilities.

THEORY

In an earlier paper (Kalaydjian, 1987), a discussion of modelling of two-phase flow was presented. It was based on the use of an averaging technique and the theory of the thermodynamics of irreversible processes. The averaging procedure consisted in defining core scale functions from their pore scale counterparts by smoothing them by taking their convolution product with a weighting function.

This method is a mathematically well-established representation of the definition of any core scale function in a *Representative Elementary Volume.* In order to get phenomenological equations such as the Darcy's equations, this averaging procedure was completed by the use of the thermodynamics of irreversible processes. This last technique is a very powerful method which consists in writing for all the phases of the system an entropy balance equation from which phenomenological equations can be derived.

A new expression of the dynamic capillary pressure has been found. Instead of the standard expression for the capillary pressure which is derived from the Laplace law, an additional term, purely of dynamic origin (it vanishes when the flow rate goes to zero), has been found and was expressed as follows:

$$P_{c_{dyn}} = P_{c_{stat}} + \lambda\, \partial(\phi s)/\partial t \qquad (1)$$

In order to cast light on the physical meaning of this coefficient, it is interesting to examine its dimensions. According to Equation (1), λ is in units of Pa.s which is exactly the dimension of a viscosity. Pore scale interpretation of the changes of capillary pressure curves has underlined the role played by viscous forces.

TEST OF THE DYNAMIC EXPRESSION OF THE CAPILLARY PRESSURE

With three experiments at hand, the verification consisted in comparing the two relatively high flow rate experiments (5 cc/hr and 15 cc/hr) with the low flow rate one (1 cc/hr) which has been checked to be identical to the static (0 cc/hr) one. As a first step, the difference between the capillary pressures was obtained. Then, at the same level on which the capillary pressure was estimated, the data on the time variation of saturation was used, *i.e.* the time derivative of these saturations at each flow rate was formed. In Figure 11 calculation of the parameter λ for the sample L13 is presented.

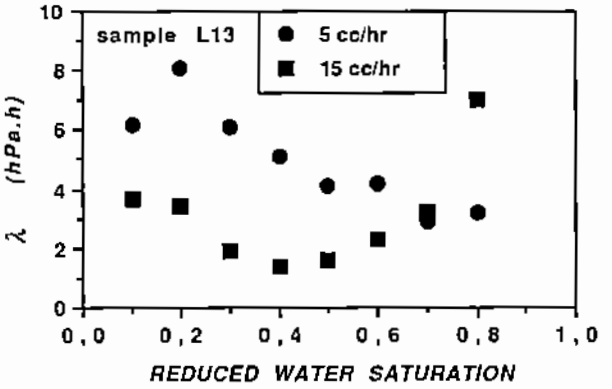

FIGURE 11 Calculation of the factor λ, (sample L13)

Two results can be observed. First of all, λ depends on the flow rate: the higher the flow rate is, the lower the parameter λ is. It appears that increasing the flow rate by a factor 3 (from 5 cc/hr to 15 cc/hr) makes λ decrease by approximately a factor 3. In that sense, we could propose an inverse proportionality with the flow rate. λ has to depend on the nature of the porous medium. The same calculation as done for the sample L13

has been carried out for the sample M5500. λ has been found to vary between 1.5 hPa.h (5 cc/hr) and 4.5 hPa.h (15 cc/hr). A dependence on the tortuosity should be investigated in a further work. Secondly, the variation of λ with saturation can be related to the changes with the flow rate of $\partial P_c/\partial s$. At 5 cc/hr, $\partial P_c/\partial s$ is monotoneous while at 15 cc/hr, $\partial Pc/\partial s$ begins by decreasing then is increasing.

The proportionality of λ with $\partial P_c/\partial s$ should be investigated.

CONCLUSIONS AND DISCUSSION

In this paper, we have shown that the imbibition capillary pressure curve depends on the flow rate. This result has been supported theoretically by use of an averaging technique coupled with the linear theory of the thermodynamics of irreversible processes. It has been found out that a term of purely dynamic origin, proportional to the partial time derivative of the saturation, had to be considered in addition to the standard quasi-static one. In order to check the new expression, an experimental study has been developed which consisted in performing waterfloods at various flow rates, recording the recovery, the total pressure drop and measurements of the capillary pressure and the saturation (by ultrasonic method) at discrete locations during the flow.

It has been found that increasing the flow rate tends to increase the capillary pressure and decrease its rate of change with saturation. This last result conforms to a decreasing impact of capillary effects when the flow rate is increased.

This new expression should lead to a more accurate modelling of spontaneous and forced imbibitions in porous media.

Finally, the new model casts light on the limits of the standard approach to model two-phase flow in porous media. It appears that it is difficult to split viscous effects and capillary effects in two separate parts: the relative permeabilities and capillary pressures. The dependence of the relative permeabilities on the flow rate has been confirmed in this study. It appears that the capillary pressure depends on the competition between viscous and capillary forces as well. This effect has been shown to affect the determination of

relative permeabilities.

Dynamic capillary pressure has thus to be taken into account to accurately model imbibition in porous media, especially when flow conditions imply sharp saturation variations as it is in heterogeneous porous media.

Acknowledgments This work was supported by EC, DG XII, Program BRITE, Project P-2289, Contract RI1B-0290-C(AM) and by the Institut Français du Pétrole. The author thanks Christian Lemaire and Françoise Deflandre for their help in the performance of the experiments.

Nomenclature

A	cross section area (m^2)
d	density
i, i=o,w	subscripts denoting oil and water phase
x,t	position and time
k	absolute permeability (m^2)
L	core length (m)
k_r	relative permeability
S	saturation (S_{or}, residual oil saturation)
P_c	capillary pressure (Pa): $P_c = P_o - P_w$
λ	Dynamic capillary pressure factor (Pa.s)
μ	viscosity (Pa.s)
ϕ	porosity

References

Bacri J.-C. and Salin D. (1989) Sound Velocity of a Sandstone Saturated with Oil and Brine at Different Conditions, *Geophysical Research Letters*, **13**, No 4, pp. 326-328.

Deflandre F. and Lenormand R. (1992) Laboratory Measurements of Oil/Water Saturations by Ultrasonic Technique, *paper presented at the 3rd European Core Analysis Symposium (EUROCAS III), Paris, September 14-16, 1992.*

Chardaire C, Chavent G., Jaffre J., Liu J. and Bourbiaux B. (1989) Simultaneous Estimation of Relative Permeabilities

and Capillary Pressure, SPE paper No 19680, *presented at the 64th Annual Technical Conference and Exhibition of the Society of Petroleum Engineers held in San Antonio, TX, October 8-11, 1989.*

Calvo A., Paterson, I, Chertcoff R., Rosen M. and Hulin J.P. (1991) Dynamic Capillary Pressure Variations in Diphasic Flows through Glass Capillaries, *J. of Colloid and Interface Science*, **14**, No 2, pp. 384-394.

Danis M. and Jacquin C. (1983) Influence du Contraste des Viscosités sur les Perméabilités Relatives lors du Drainage. Expérimentation et Modélisation, *Rev. Inst. Franç. Pétrole*,**38**, 6, Nov.-Dec., pp. 723-733.

Dullien F.A.L., Allsop H.A., Chatzis I., and Macdonald I.F. (1990) *Can J.P.T.*, **29**, No 4, p. 63.

Hoyos M., Moulu J.-C., Deflandre F. and Lenormand R. (1990) Ultrasonic Measurement of the Bubble Nucleation rate during Depletion Experiments in a Rock Sample, SPE paper No 20525, *presented at the 65th Annual Technical Conference and Exhibition of the Society of Petroleum Engineers held in New-Orleans, Sept. 23-26, 1990.*

Kalaydjian F. (1987) A Macroscopic Description of Multiphase Flow in Porous Media Involving Space-time Evolution of Fluid/Fluid Interface, *Transp. in Porous Media*, **2**, 6, pp. 537-552.

Kalaydjian F. (1990) Origin and Quantification of Coupling berween Relative Permeabilities for Two-Phase Flows in Porous Media, *Transp. in Porous Media*, **5**, pp. 215-229.

Kalaydjian F. and Bourbiaux B. (1989) Viscous Coupling between Fluid Phases for Two-Phase Flow in Porous Media: Theory versus Experiment, *paper presented at the 5th European Symposium on Improved Oil Recovery, Budapest, 25-27 April 1989.*

Legait B., Sourieau P. and Combarnous M. (1983) Inertia Viscosity, and Capillary Forces during Two-Phase Flow in a Constricted Capillary Tube, *J. Coll. Interface Sci.*, **91**, No 2, pp. 400-411.

Ngan C.G. and Dussan E.B. (1982) On the nature of the dynamic contact angle: an experimental study, J. Fluid Mech., **118**, pp. 27-40.

Tsakiroglou C.D and Payatakes A.C. (1991) Effects of Pore-Size Correlations on Mercury Porosimetry Curves, *J. of Colloid and Interface Sci.*, **146**, No 2, pp. 479-494.

Fluid Saturation